Journal of Pharmaceutical and Biomedical Analysis 235 (2023) 115611

Contents lists available at ScienceDirect

Journal of Pharmaceutical and Biomedical Analysis

journal homepage: www.journals.elsevier.com/journal-of-pharmaceutical-and-biomedical-analysis

UPLC-ESI-QTOF-MS assisted targeted metabolomics to study the enrichment of vinca alkaloids and related metabolites in *Catharanthus roseus* plants grown under controlled LED environment

Katalin Nagy [a,b], Éva Darkó [a], Gabriella Szalai [a], Tibor Janda [a], Zsuzsa Jókai [b], Márta Ladányi [c], Mohamed Ramadan Rady [d], Mihály Dernovics [a,*]

[a] Department of Plant Physiology and Metabolomics, Agricultural Institute, Centre for Agricultural Research, ELKH, Brunszvik u. 2., Martonvásár 2462, Hungary
[b] Department of Food Chemistry and Analytical Chemistry, Institute of Food Science and Technology, Hungarian University of Agriculture and Life Sciences, Villányi út 29-43., Budapest 1118, Hungary
[c] Department of Applied Statistics, Institute of Mathematics and Basic Science, Hungarian University of Agriculture and Life Sciences, Villányi út 29-43., Budapest 1118, Hungary
[d] Department of Plant Biotechnology, National Research Centre, 33 El Behouth st., Dokki, Giza P.O. 12622, Egypt

ARTICLE INFO

Keywords:
Vinblastine
Vincristine
Targeted metabolomics
MANOVA
Games-Howell's post hoc test
VIP
UPLC
Periwinkle

ABSTRACT

Enrichment of pharmaceutically important vinca alkaloids, vinblastine and vincristine, in the leaves of Madagascar periwinkle (*Catharanthus roseus*) plants through different pre- or postharvest treatments or cultivation conditions, e.g., exposing the plants to UV-irradiation, has been in focus for decades. Controlled LED environment in the visible light range offers the possibility of monitoring the changes in the concentration of metabolites in the vinca alkaloid-related pathway without involving UV-related abiotic stress. In the frame of our targeted metabolomics approach, 64 vinca alkaloids and metabolites were screened with the help of a UPLC-ESI-QTOF-MS instrumental setup from the leaf extracts of *C. roseus* plants grown in chambers under control (medium light), low light, and high blue / high red/ high far-red conditions. Out of the 14 metabolites that could be assigned either unambiguously with authentic standards or tentatively with high resolution mass spectrometry-based methods, all three dimer vinca alkaloids, that is, 3',4'-anhydrovinblastine, vinblastine and vincristine showed an at least nine-fold enrichment under high blue irradiation when compared with the control conditions: final concentrations of 961 mg kg^{-1} dry weight, 33.8 mg kg^{-1} dry weight, and 11.7 mg kg^{-1} dry weight could be achieved, respectively. As supported by multivariate statistical analysis, the key metabolites of the vinca alkaloid pathway were highly represented among the metabolites that were specifically stimulated by high blue light application.

1. Introduction

There are roughly 300.000 plant species in the world, but only about 30 % of them were used in scientific investigation [1]. As a whole, there are more than 100 known plant-derived compounds with potential medical applications [2], and many of them fall under the category of traditional medicine. However, some of them have potent effects and should only be used with care and in accordance with dosage guidelines. In the latter case, it is crucial to ensure the constant quality of the herbal drugs used as raw materials.

A complicated issue with regard to the quality control of the raw materials and the derived products is created by the high degree of variability in the quality of the plants raw material. Most countries have established systems for the quality control of herbal drugs. Legally recognized medications must pass identification and purity tests and have their primary bioactive components' standard values determined, as well as assurances of plant preservation and microbiological purity. Indeed, straightforward guidelines and regulations must be established; this work is currently being carried out either by international organizations or at national levels (IFPMA, WHO [3]). As a result, the quantitative range of secondary metabolites, which can be thought of as various stations of the biosynthetic pathways and to be used medicinally as bioactive components, can be very broad. Thus, maintaining consistent raw material quality in traditional cultivation is a very difficult task.

* Corresponding author.
E-mail address: dernovics.mihaly@atk.hu (M. Dernovics).

https://doi.org/10.1016/j.jpba.2023.115611
Received 26 May 2023; Received in revised form 28 July 2023; Accepted 29 July 2023
Available online 29 July 2023

The tight regulation of cultivation conditions may be the answer to this issue. Plant properties, including modifications in their metabolomic pathways, are strongly influenced by cultivation technology and external environmental factors in addition to the inherent variability of individual plants. To ensure the quality with the highest possible yield, many plants including herbs are cultivated under artificial environmental conditions, where the environmental parameters (temperature, light, humidity) can be fixed or changed adequately according to the plant species and growing requirements. In modern indoor cultivation systems, LED (light-emitting diode) lighting technology can ensure adequate light intensity and spectral composition for the optimal growth and development of plants [4–6]. With LED lighting assistance, plants can be "tuned" to accumulate specific secondary metabolites by interfering with their biosynthetic pathways. This may be a practical method for synthesizing compounds whose total synthesis has not yet been elaborated through preparative organic chemistry or a more environmentally friendly method than conventional organic chemical synthesis. Primarily in the food industry and horticulture, but also in the pharmaceutical industry, many efforts have been made this way to influence the production of useful secondary metabolites in various plants [7,8].

Apocynaceae family plant *Catharanthus roseus* (L.) G. Don, formerly known as *Vinca rosea*, is a well-known ornamental and medicinal plant. Out of the eight *Catharanthus* species, only *C. roseus* is widely distributed throughout the world. Two color varieties (pink and white) are found in the natural state [2] but many others (e.g., blush pink with red eye, crimson, and white with red eye) are listed as commercially available seed hybrids. Including these plants in a broad screening program was one of the options for the search for bioactive plant components that can be used as medicines, but it depends on the availability of sufficient funding and suitable predictable bioassay systems. Concerning *C. roseus*, vincristine sulfate and vinblastine sulfate are two of the few significant effective medications that entered the market using this methodology [1]. Vinblastine and vincristine, the two most valuable vinca alkaloids, are frequently used in combination chemotherapy for choriocarcinoma, lung cancer, acute leukemia, and Hodgkin's disease along with other anti-tumor medications [9]. As recently summarized by Kumar et al. [10], the market prices for the supply of vinblastine and vincristine is estimated at $2 million/kg and $15 million/kg, respectively, and their supply are limited by the availability of the plant worldwide.

C. roseus has been targeted with LED lighting for approximately a decade to try to provide stable drug supply of vinca alkaloids. The main goal of the studies was to optimize the lighting treatment for the maximum production of the precursors of vinblastine, i.e., vindoline and catharanthine. Fukuyama et al. [11] discovered a significant increase in plant growth parameters when they were exposed to red light, but they did not see any significant differences in the quantity of vindoline or catharanthine the plants produced under the various sets of illumination. They also determined [12] that the red light intensity that could maximize the vindoline and catharanthine production per plant was between 150 and 300 μmol m^{-2} s^{-1}. However, the application of red light did not promote vinblastine production. To overcome this, by exposing the plants grown under red light to UV-A radiation, it was possible to increase the amount of vinblastine in the leaves of *C. roseus* [13], and the application of UV-B also induced the accumulation of alkaloids [14]. However, the application of UV irradiation may provoke some unforeseen physiological effects such as decreased average internode length, and accordingly, more gentle methods to increase vinca alkaloid concentration would be advantageous [15].

From a clinical point of view it is critically necessary to determine the concentration levels of vinca alkaloids in raw *C. roseus*, in *C. roseus*-derived pharmaceutical products as well as in human serum samples. Several analytical techniques have been published recently for determining the vinca alkaloids in *C. roseus* [16,17]. In comparison to others, such as gas chromatography and capillary electrophoresis chromatography, high-performance liquid chromatography (HPLC) combined with a diode array detector (DAD), fluorescence detector (FLD), and mass

Table 1
List of vinca alkaloids and metabolically-related compounds targeted in the study.

Compound	Neutral formula	Neutral mass	Characteristic adduct in ESI-MS
(3 R)− 3-Hydroxy-1,2-didehydro-2,3-dihydrotabersonine	C21H24N2O3	352.1787	–
(3 R)− 3-Hydroxy-16-methoxy-1,2-didehydro-2,3-dihydrotabersonine	C22H26N2O4	382.1893	–
(3 R)− 3-Hydroxy-2,3-dihydrotabersonine	C21H26N2O3	354.1943	–
(S)− 8-Oxocitronellyl enol	C10H16O2	168.1150	–
10-Deoxygeniposidic acid	C16H22O9	358.1264	–
16-Hydroxytabersonine	C21H24N2O3	352.1787	$[M+H]^+$
16-Methoxy-2,3-dihydro-3-hydroxytabersonine	C22H28N2O4	384.2049	–
16-Methoxytabersonine	C22H26N2O3	366.1943	$[M+H]^+$
19-Hydroxytabersonine	C21H24N2O3	352.1787	$[M+H]^+$
19-*S*-vindolinine	C25H32N2O6	456.2260	$[M+H]^+$
3',4'-Anhydrovinblastine	C46H56N4O8	792.4098	$[M+2H]^{++}$
4,21-Dehydrogeissoschizine	C21H23N2O3	351.1709	$[M+H]^+$
7-Deoxyloganate	C16H24O9	360.1420	–
7-Deoxyloganetate	C10H14O4	198.0892	–
7-Deoxyloganetic alcohol	C10H16O3	184.1099	–
7-Deoxyloganetin	C11H16O4	212.1049	–
7-Deoxyloganin	C17H26O9	374.1577	–
8-Hydroxygeraniol	C10H18O2	170.1307	–
8-Oxogeranial	C10H14O2	166.0994	–
Ajmalicine	C21H24N2O3	352.1787	$[M+H]^+$
Ajmaline	C20H26N2O2	326.1994	$[M+H]^+$
Alstonine	C21H20N2O3	348.1474	$[M+H]^+$
Asperuloside	C18H22O11	414.1162	$[M+H]^+$
Catharanthamine	C46H56N4O9	808.4047	–
Catharanthine	C21H24N2O2	336.1838	$[M+H]^+$
Cathenamine	C21H22N2O3	350.1630	–
cis-trans-Nepetalactol	C10H16O2	168.1150	–
Deacetylvindoline	C23H30N2O5	414.2155	$[M+H]^+$
Desacetoxyvindoline	C23H30N2O4	398.2206	–
Echitovenine	C23H28N2O4	396.2049	$[M+H]^+$
Geissoschizine	C21H24N2O3	352.1787	$[M+H]^+$
Geniposidic acid	C16H22O10	374.1213	$[M-H]^-$
Gentiopicrin	C16H20O9	356.1107	$[M+Na]^+$
Geraniol	C10H18O	154.1358	$[M+H]^+$
Horhammericine	C21H24N2O4	368.1736	$[M+H]^+$
Iridotrial	C10H14O3	182.0943	–
Lochnericine	C21H24N2O3	352.1787	$[M+H]^+$
Lochnerinine	C22H26N2O4	382.1893	–
Loganic acid	C16H24O10	376.1370	$[M+H]^+$, $[M-H]^-$
Loganin	C17H26O10	390.1526	$[M+H]^+$, $[M-H]^-$
Minovincinine	C21H26N2O3	354.1943	$[M+H]^+$
Norajmaline	C19H24N2O2	312.1838	–
Norseredamine	C20H24N2O2	324.1838	$[M+H]^+$
Raucaffricine	C27H32N2O8	512.2159	$[M+H]^+$
Reserpine	C33H40N2O9	608.2734	$[M+H]^+$
Sarpagine	C19H22N2O2	310.1681	–
Secologanate	C16H22O10	374.1213	$[M-H]^-$
Secologanin	C17H24O10	388.1370	$[M+Na]^+$
Serpentine	C21H20N2O3	348.1474	$[M+H]^+$
Stemmadenine	C21H26N2O3	354.1943	–
Strictosidine	C27H34N2O9	530.2264	$[M+H]^+$
Strictosidine aglycone	C21H24N2O4	368.1736	–
Tabersonine	C21H24N2O2	336.1838	$[M+H]^+$
Tetrahydroalstonine	C21H24N2O3	352.1787	$[M+H]^+$
Vellosimine	C19H20N2O	292.1576	$[M+H]^+$
Vinblastine	C46H58N4O9	810.4204	$[M+H]^+$
Vincadifformine	C21H26N2O2	338.1994	$[M+H]^+$
Vincristine	C46H56N4O10	824.3996	$[M+H]^+$
Vindoline	C25H32N2O6	456.2260	$[M+H]^+$
Vindolinine	C21H24N2O2	336.1838	$[M+H]^+$
Vindorosine	C24H31N2O5	427.2233	$[M+H]^+$
Vinorine	C21H22N2O2	334.1681	–
Vomilenine	C21H22N2O3	350.1630	$[M+H]^+$
Yohimbine	C21H26N2O3	354.1943	$[M+H]^+$

Table 2
Experimental settings of the LED treatment.

No.	Type	SUM PPFD (μmol m^{-2} s^{-1})	Blue %	Green %	Red %	Far-red %
1	High blue	350	43	15	41	1
2	High red	350	11	15	73	1
3	High far-red	350	20	15	44	21
4	Medium light (control)	350	20	15	64	1
5	Low light	115	20	15	64	1

Fig. 1. *C. roseus* plants during the LED treatment (No. 5 low light on the left side and No. 1 high blue to the right).

spectrometry (MS) were the most frequently used methods. Especially the latter has been regarded as the crucial technique, taking into account the lack of authentic standards for several of the vinca alkaloid-related secondary metabolites [18]. The simultaneous quantitative determination of known target components in very low concentrations for which authentic standards are commercially available can be accomplished using LC-ESI-MS/MS analysis; however, further members of the biosynthetic pathway can only be determined with some uncertainty and quantified to another component [19,20]. For the detection and assignment of secondary plant metabolites without authentic standards, LC-coupled high resolution mass spectrometry setups (LC-ESI-/Q/TOF-MS, LC-ESI-Orbitrap-MS) offer a straightforward and even retrospective analysis ready alternative to the quantitative and qualitative techniques now in use. Also, together with elucidating the isotopologue profiles of unknown components, accurate mass determination reduces the ambiguity in spectral interpretation, allowing for the determination of the metabolic profile of the plant. However, there have been relatively few publications so far on the vinca alkaloid metabolome and none of them attempted to cover the related biosynthetic pathway [21–23].

Our research aimed to launch a targeted metabolomic study on the accumulation of vinca alkaloids and their related biosynthetic surrogates in the leaves of *C. roseus* grown under various artificial (LED) lighting conditions. To achieve this, a dataset of vinca analytes with their elemental composition and accurate mass information was set up (Table 1), together with the favoured ionization mode to facilitate the compound assignment. Besides multivariate statistical approaches, absolute and relative quantifications were also carried out to map the influence of light intensity as well as the effects of red, far-red or blue lights on the main vinca metabolites, namely 3',4'-anhydrovinblastine, vinblastine and vincristine.

Table 3
UPLC gradient conditions.

Gradient conditions **Eluent 'A': water with 0.1% V/V formic acid** **Eluent 'B': acetonitrile with 0.1% V/V formic acid**			
Time (min)	Flow rate (mL min^{-1})	A%	B%
0.0	0.4	95	5
0.5	0.4	95	5
8.0	0.4	82	18
12.0	0.4	60	40
15.0	0.4	20	80
16.0	0.4	0	100
18.0	0.4	0	100
19.0	0.4	95	5
22.0	0.4	95	5

2. Materials and methods

2.1. Plant materials and growth conditions

300 seedlings were raised from seeds (Rédei Kertimag Zrt., Réde, Hungary; undisclosed cultivar) for two months in a PGR-15 growth chamber (Conviron Ltd., Winnipeg, Canada) under uniform growth conditions at 26/20 °C day/night temperature, 300 μmol m^{-2} s light intensity provided by metal halide lamps with 16/8 h photoperiod and 70–75 % relative humidity.

After two months, seedlings were transferred to the LED chambers and were exposed to different light treatments (Table 2) for two weeks. For each LED set-up, 12–12 seedlings were taken, as presented in Fig. 1. After two weeks of irradiation, five plants from each LED set-up were taken for the vinca alkaloid analysis: four fully developed leaves were taken from each plant from the top of the plants. The leaf samples were frozen in liquid nitrogen and then stored at –80 °C until further sample preparation.

2.2. Chemicals and reagents

As for authentic standards, vincristine sulfate (≥ 99 %) and vinblastine sulfate (≥ 97 %) were purchased from the Merck-Sigma group (Darmstadt, Germany). Sample preparation was carried out with UPLC gradient grade methanol and HPLC grade n-hexane, both obtained from VWR (Radnor, PA, USA). Deionized water (18.2 MΩ*cm) was obtained from a Millipore purification system (Merck-Millipore; Darmstadt, Germany). For the LC-MS analyses, UPLC-MS-grade acetonitrile and MS-grade formic acid were used (VWR).

2.3. Sample preparation

Leaf samples were powdered in liquid nitrogen in a mortar with a pestle. 0.2 g sample was weighted and the extraction was performed with 2 × 1 mL MeOH:H_2O (2:1, V:V) for 2 min each in a 1600 Mini-G®—Automated Tissue Homogenizer and Cell Lyser (SPEX; Rickmansworth, UK) at 1250 rpm. After centrifugation (10 min, 4 °C, 16500 *g*), the supernatants were collected. The combined supernatants were liquid-liquid partitioned by adding 1.0 mL of n-hexane to remove carotenoids. Before the LC-MS analyses, the methanol:water phase was filtered through 0.22 μm PTFE syringe filter, and 0.5 mL of filtered samples was diluted both with 0.5 mL MQ water containing 0.2 % V/V formic acid and with 4.5 mL MQ water containing 0.11 % V/V formic acid to reach either a 2-fold or a 10-fold dilution, respectively.

2.4. Metabolomics and multivariate statistical analysis

The analysis was carried out with a Waters Acquity I-class ultra-performance liquid chromatography (UPLC) system equipped with a PDA detector, which was coupled to a Vion ESI-IMS-QTOF-MS instrument (Waters; Milford, MA, USA). Separation was performed on a BEH-

Table 4
ESI-IMS-QTOF-MS parameters applied during the study.

Detector 1	PDA - 220–600 nm; 20 scans/s at 2.4 nm resolution
Detector 2	Vion IMS QTOF MS with ESI ion source
Resolution	> 40 000 (calculated for leucine enkephalin)
Capillary voltage	0.5 kV
Polarity	negative and positive
Source temperature	120 °C
Desolvation temperature	550 °C
Nebulizer gas	6.5 bar N_2
Cone gas voltage	30 V
Desolvation gas flow	1000 L h^{-1} N_2
Cone gas flow	150 L h^{-1} N_2
Collision gas flow	0.15 mL min^{-1} Ar 5.0
IMS	ON
MS scan	*m/z* 90 – 2000
MS scan time	0.4 s
Lock mass	ON
MS/MS scan	*m/z* 50 – 2000
MS/MS collision energy	individually optimized
MS^E low collision energy	6.0 eV
MS^E high collision energy ramp	20.0–30.0 eV

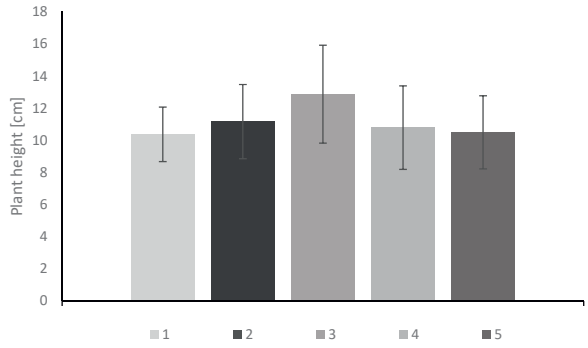

Fig. 2. Plant heights after two weeks of treatment. [1 – high blue, 2 – high red, 3 – high far-red, 4 – medium light (control), 5 – low light].

C_{18} reversed phase (RP) UPLC column (100 mm × 2.1 mm × 1.7 μm; Waters) at 40 °C. For gradient elution, water and acetonitrile containing 0.1 % V/V formic acid were used. The injected sample volume was 1 μL. The applied gradient and the UPLC-ESI-IMS-QTOF-MS parameters are described in Tables 3 and 4. To demonstrate the applicability of the method, a validation study was carried out, comprising of the assessment of specificity/selectivity, linearity, precision, analytical range, the limits of detection (LOD) and quantification (LOQ), and the matrix effect. For the quantification of the samples, the standard addition method was used to set up the calibration, with authentic standards of vinblastine and vincristine. The concentration of 3',4'-anhydrovinblastine was determined against the authentic standard of vinblastine, which can therefore be regarded as a semi-quantitative approach for this compound.

Data processing and multivariate statistical analyses were performed using UNIFI (version 1.9.4; Waters), Progenesis QI (for Principle Component Analysis /PCA/; Version 27.26.1020; Nonlinear Dynamics, Quayside, Newcastle Upon Tyne, UK), EZinfo (for Partial Least Squares Discriminant Analysis /PLS-DA/, S-plot and variable importance /VIP/ analyses; version 3.0.3; UMetrics AB, Umeei, Sweden) and R (version 4.1.2; R Core Team; Vienna, Austria) software packages. The height of the plants (n = 12 in each experimental group) was compared by one-way ANOVA. The model residuals were tested for normality and homogeneity of variances by Shapiro-Wilk's and Levelene' tests, respectively ($p > 0.05$). The effect of LED parameters on vinca alkaloids and metabolites was tested by one-way MANOVA. During this process, vinblastine was transformed by 1/sqrt(x) to ensure the distribution requirement. The normality of the residuals was accepted according to Shapiro-Wilk's test ($p > 0.05$). The homogeneity of variances was checked by Levene's test; it was violated in cases of catharantine and vincristine. With a significant overall MANOVA result, one-way ANOVA tests were run with Bonferroni's correction to avoid familywise error rate inflation. In cases where a significant factor effect was detected, pairwise comparisons were made using Games-Howell's post hoc test, which can manage the homoscedasticity violation.

3. Results and discussion

Plant height was taken as the primary indication of phenotypic differences in the function of light conditions. As presented in Fig. 2, plants exposed to high far-red irradiation (group No. 3) were considerably higher than in the other groups, but the effect was not significant based on one-way ANOVA ($F(4;55)= 2.12$, $p = 0.09$). Generally, the higher plant length is consistent with the effect of far-red light that can stimulate stem elongation in plants based on the mechanism called shade avoidance syndrome [24]. This observation cannot be directly collated with former studies on *C. roseus* [11,12]. Indeed, in the studies of Fukuyama et al., illumination was only applied in the visible range and the treatment with red light resulted in a significant increase in plant height. In our experiments, high visible red setting (group No. 2) did not result in significantly different plant height values. Indeed, none of the groups had any significant difference in this parameter showing that a

Table 5
Overview of the unambiguously (vincristine and vinblastine) or tentatively identified components of the indole alkaloid biosynthesis pathway in *C. roseus* leaves. (*) VIP scores of alstonine and serpentine could not be determined because of their close chromatographic elution. (#) Not analysed in the positive ion mode. VIP numbers in italics refer to the 10-fold diluted samples.

No.	Component name	Elemental composition (neutral)	Detected as	Theoretical *m/z*	Experimental *m/z*	Difference, ppm	RT, min	VIP (group #1 vs. #4)
1	19-*S*-vindolinine	C21H24N2O2	$[M+H]^+$	337.1911	337.1916	1.48	7.06	3.0
2	3',4'-Anhydrovinblastine	C46H56N4O8	$[M+2H]^{++}$	397.2122	397.2129	1.76	11.74	*32.3*
3	Alstonine	C21H20N2O3	$[M+H]^+$	349.1547	349.1554	2.00	10.65	–*
4	Catharanthine	C21H24N2O2	$[M+H]^+$	337.1911	337.1909	-0.59	10.41	*<2*
5	Deacetylvindoline	C23H30N2O5	$[M+H]^+$	415.2228	415.2231	0.72	10.13	*5.3*
6	Loganic acid	C16H24O10	$[M-H]^-$	375.1297	375.1301	1.07	3.17	#
7	Secologanin	C17H24O10	$[M+Na]^+$	411.1262	411.1267	1.22	6.64	6.6
8	Serpentine	C21H20N2O3	$[M+H]^+$	349.1547	349.1543	-1.15	10.46	-*
9	Strictosidine	C27H34N2O9	$[M+H]^+$	531.2337	531.2339	0.38	9.63	*<2*
10	Vinblastine	C46H58N4O9	$[M+2H]^{++}$	406.2175	406.2176	0.25	11.12	6.6
11	Vincadifformine	C21H26N2O2	$[M+H]^+$	339.2067	339.2070	0.88	10.55	*<2*
12	Vincristine	C46H56N4O10	$[M+2H]^{++}$	413.2071	413.2076	1.21	10.72	2.9
13	Vindoline	C25H32N2O6	$[M+H]^+$	457.2333	457.2327	-1.31	11.25	*2.6*
14	Vindolinine	C21H24N2O2	$[M+H]^+$	337.1911	337.1915	1.19	8.01	<2

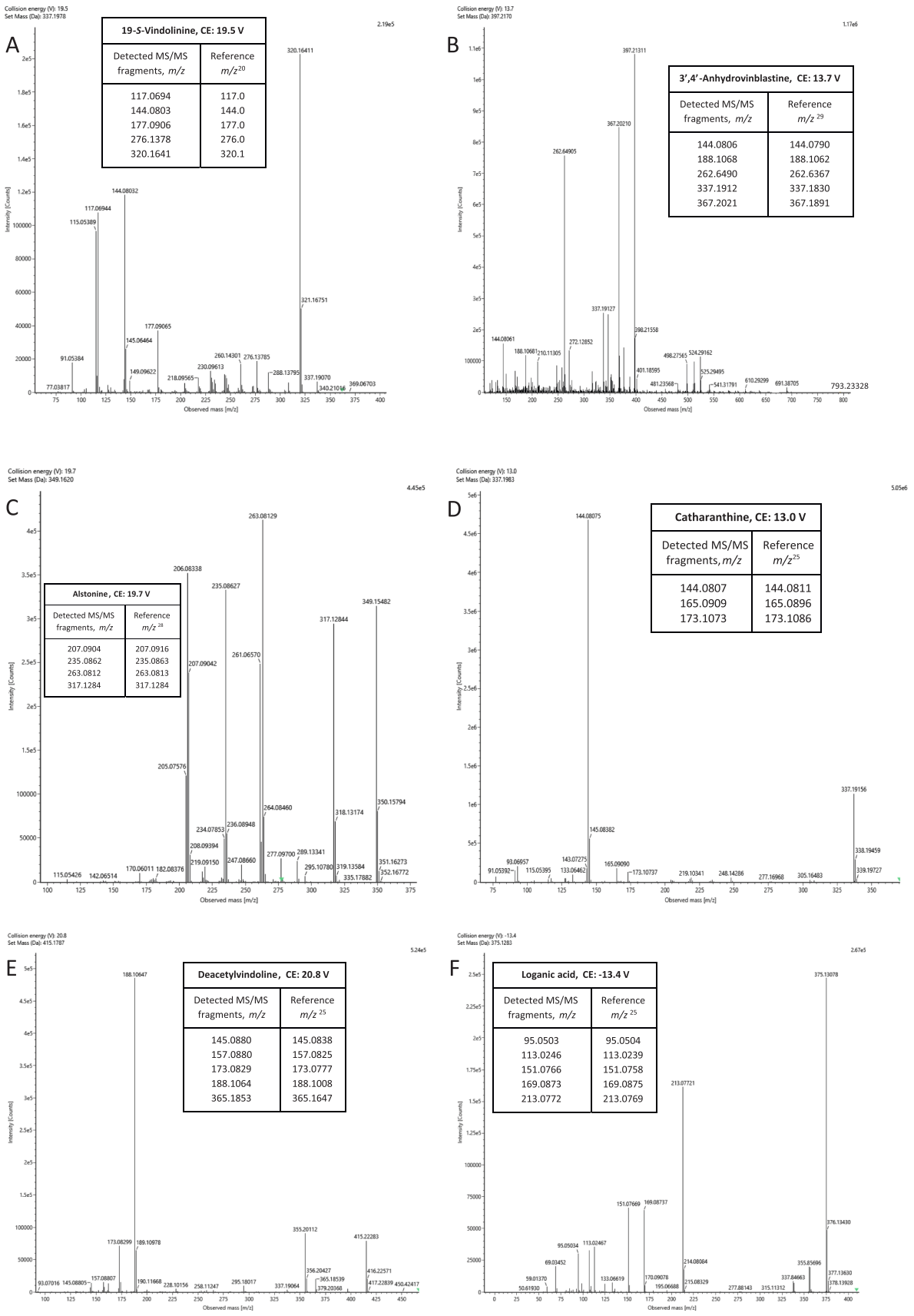

Fig. 3. MS/MS spectra of the tentatively identified compounds with reference *m/z* data in the insets. [A – 19-*S*-Vindolinine, B – 3',4'-Anhydrovinblastine, C – Alstonine, D – Catharanthine, E – Deacetylvindoline, F – Loganic acid, G – Secologanin, H – Serpentine, I – Strictosidine, J – Vincadifformine, K – Vindoline, L – Vindolinine]. 'CE' refers to collision energy.

G

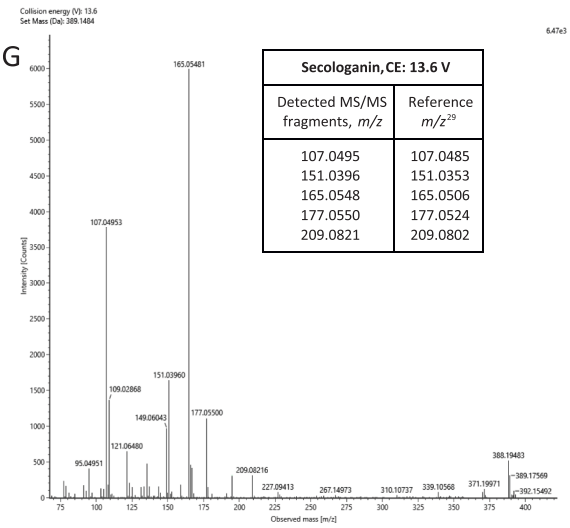

Secologanin, CE: 13.6 V	
Detected MS/MS fragments, *m/z*	Reference *m/z*[29]
107.0495	107.0485
151.0396	151.0353
165.0548	165.0506
177.0550	177.0524
209.0821	209.0802

H

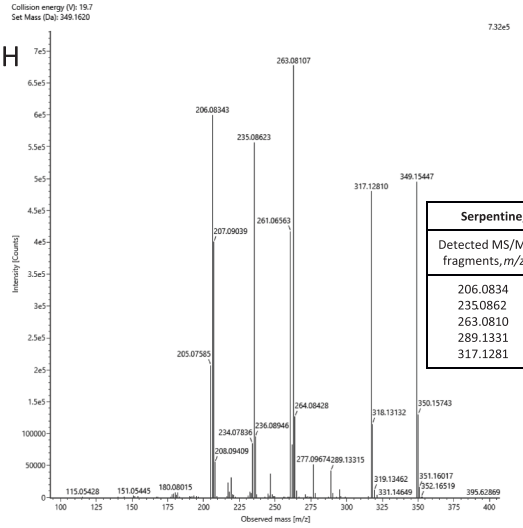

Serpentine, CE: 19.7 V	
Detected MS/MS fragments, *m/z*	Reference *m/z*[26]
206.0834	206.0821
235.0862	235.0841
263.0810	263.0789
289.1331	289.1290
317.1281	317.1252

I

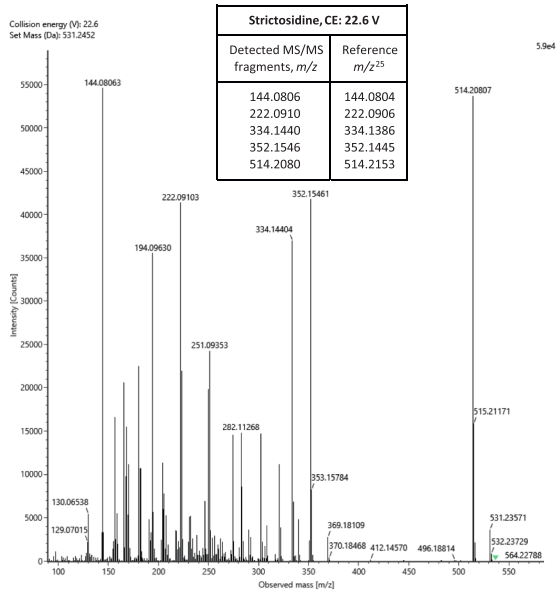

Strictosidine, CE: 22.6 V	
Detected MS/MS fragments, *m/z*	Reference *m/z*[25]
144.0806	144.0804
222.0910	222.0906
334.1440	334.1386
352.1546	352.1445
514.2080	514.2153

J

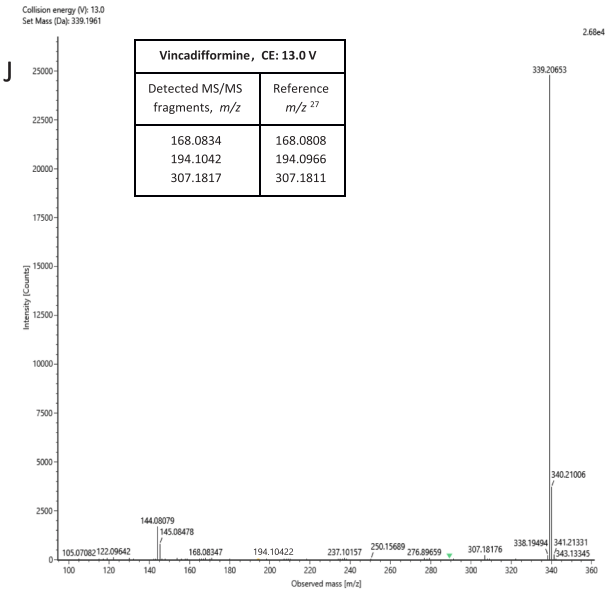

Vincadifformine, CE: 13.0 V	
Detected MS/MS fragments, *m/z*	Reference *m/z* [27]
168.0834	168.0808
194.1042	194.0966
307.1817	307.1811

K

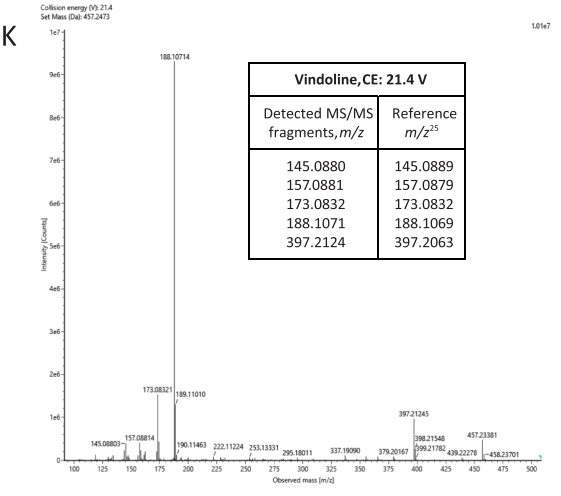

Vindoline, CE: 21.4 V	
Detected MS/MS fragments, *m/z*	Reference *m/z*[25]
145.0880	145.0889
157.0881	157.0879
173.0832	173.0832
188.1071	188.1069
397.2124	397.2063

L

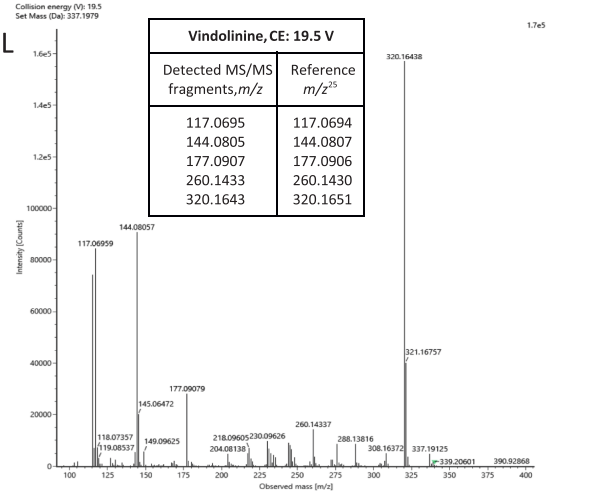

Vindolinine, CE: 19.5 V	
Detected MS/MS fragments, *m/z*	Reference *m/z*[25]
117.0695	117.0694
144.0805	144.0807
177.0907	177.0906
260.1433	260.1430
320.1643	320.1651

Fig. 3. (*continued*).

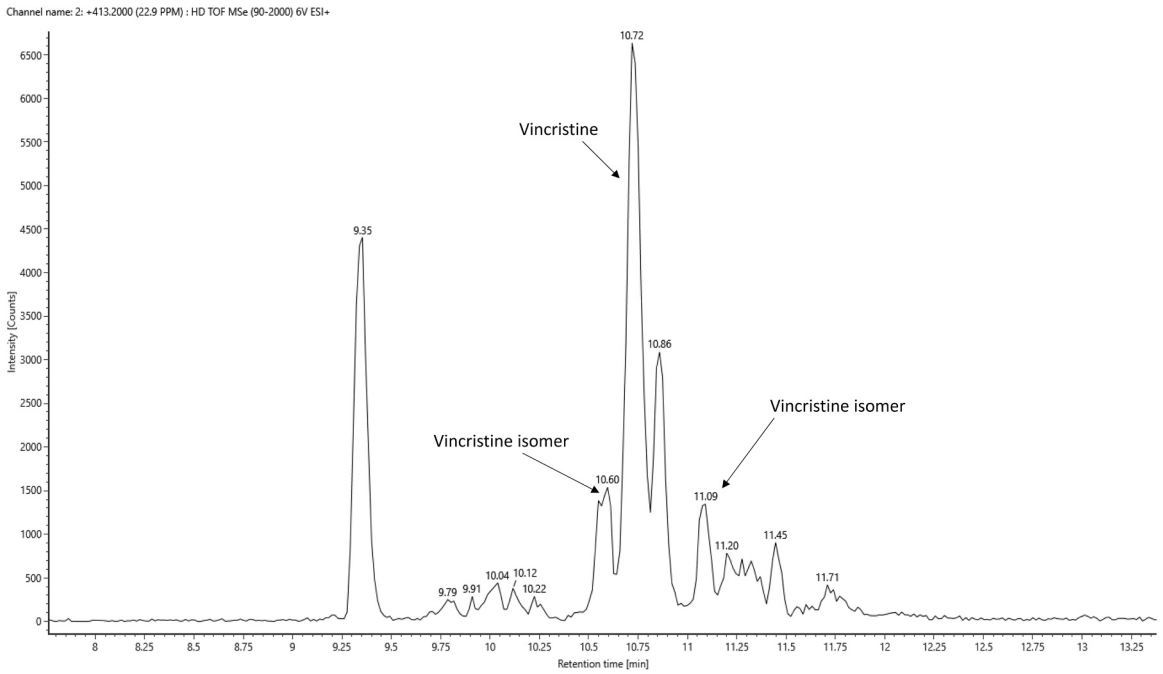

Fig. 4. Extracted ion chromatogram of vincristine, detected as $[M+2H]^{++}$ in the positive ESI mode. The retention time of the analyte (RT=10.72 min) was validated with the use of an authentic standard.

2-week long light treatment was not enough for resulting in significant differences in growth.

Indole alkaloids, their metabolites and precursors were screened for in the full scan UPLC-ESI-QTOF-MS spectra based on a list of 64 analytes associated to vinca alkaloid synthesis (Table 1). Apart from vincristine and vinblastine, the other components were tentatively identified with the help of their high-resolution MS spectra, high-resolution MS/MS spectra and retention order. Finally, 14 components of the related pathway could be assigned from the 64 targeted analytes (Table 5 and Fig. 3) on the basis of authentic standards (vinblastine, vincristine), of the reference MS/MS spectra from the MoNA database (catharanthine, deacetylvindoline, loganic acid, strictosidine, vindoline, vindolinine) [25] and of the studies of Kumar et al. (serpentine) [26], Abouzeid et al. (vincadifformine) [27], Wang et al. (alstonine) [28], Pan et al. (3', 4'-anhydrovinblastine, secologanin) [29], Eng et al. [30], and Ferreres et al. (19-*S*-vindolinine) [20]. The use of the authentic standard of vincristine was of utmost importance due to the detection of abundant vincristine isomers (see Fig. 4 for the extracted ion chromatogram of the accurate mass of vincristine). Accordingly, the resolution of isomers from the authentic compound with the help of UPLC was a key feature for the accurate quantification of vincristine. The Electronic Supplementary Information also presents all full scan MS spectra (Fig. 3 and ESI-Fig. 1-14) and the extracted ion chromatograms (ESI-Figures 15–18) of the 14 analytes assigned in the study that are shown framed in Fig. 5. Some of the metabolites of the indole alkaloid pathway (see the unframed compounds) could not be unambiguously detected in any of the samples, because of either inadequate retention on the applied C_{18} column, low concentration hampering high quality MS/MS acquisition, or the lack of authentic standards that would have been required to assign the target analytes among the series of isomers.

The performance characteristics was checked in the case of external calibration as well as standard addition method both for vinblastine and vincristine (Table 6). The analytical range for external calibration was 10–250 ug L^{-1}; for the standard addition process, the range of 25–100 ug L^{-1} was used. Signal enhancement was detected for both vincristine and vinblastine (Table 6), however, the calculated matrix effect never exceeded 10 %. As a result, while external calibration could have been still an appropriate option, standard addition was finally addressed for the more accurate quantification.

Light dependence of the production of identified or assigned indole alkaloids was determined by statistical analyses that were conducted in two main ways. First, the overall MANOVA was calculated on the abundances of target analytes, and the result was significant (the unexplained variance rate: Wilk's lambda < 0.001, $p < 0.001$). The follow-up univariate ANOVA tests with Bonferroni's correction revealed significant factor effect in case of loganic acid, 3',4'-anhydrovinblastine, vinblastine, vincristine, vindolinine and 19-*S*-vindolinine ($F(4;20) > 6.01$, $p < 0.01$). For vindoline, catharantine and secologanin, the factor effect was slightly significant with F(1:20) values in between 3.3 and 4.9 (Bonferroni's: $0.05 < p < 0.1$), while it was insignificant for strictosidine, deacetylvindoline, and vincadifformine ($F(4;20) < 2.96$, $p > 0.4$).

Finally, the Games-Howell's pairwise comparison resulted in the directly comparable results of the five different light treatments (ESI-Table S1). Although the amount of 3',4'-anhydrovinblastine was significantly higher under blue light and at low light intensity than at other spectral combination, the two main precursors of 3',4'-anhydrovinblastine, that is, catharanthine and vindole did not present significant changes at any light intensity and spectral combination (ESI-Table S1, ESI-Figs. 19–30).

Fukuyama et al. [12] studied the effect of red-light intensity on the accumulation of vindoline and catharanthine and they found that the highest alkaloid concentration was detected at low 150 μmol m^{-2} s^{-1} light intensity as compared to 300 or 600 μmol m^{-2} s^{-1}. This result is in accordance with our finding that the accumulation of alkaloids was higher at lower light intensity. However, a highly significant effect was induced when blue light was used.

The concentrations of vinblastine, vincristine and 3',4'-anhydrovinblastine were significantly the highest when high proportion of blue light was used (group No. 1). It provided a remarkable, up to 15-fold increase in the concentration of these key vinca alkaloids as compared to other spectral combinations. This increase was as significant as was found by Fukuyama et al. [13] under UV-A treatment or under Yu et al. [31] by UV-B treatment. In the former study, the blue light also increased the vinblastine content, but not to the extent experienced under UV-A irradiation. Since the UV treatments have negative

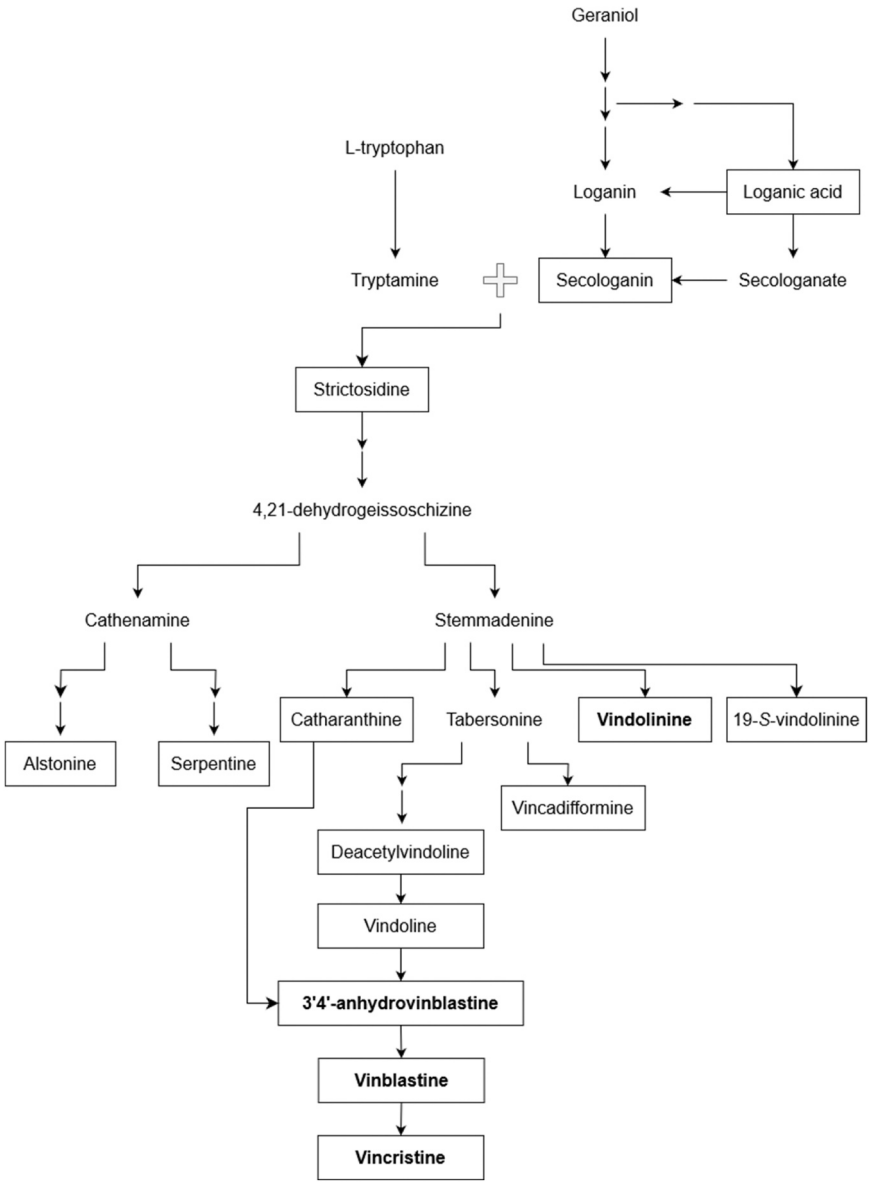

Fig. 5. Schematic diagram of the indole alkaloid biosynthesis pathway [30,35]. The framed components could be identified in the analyzed samples. The components that showed significantly higher abundance as a result of the high blue LED treatment are marked in bold.

Table 6
Performance characteristics of the UPLC-MS/MS method. (a) Limit of detection; (b) limit of quantification.

		Regression equation		LOD[a] [ug L^{-1}]	LOQ[b] [ug L^{-1}]	Matrix effect
Vinblastine	External calibration	y = 3.6459x	R^2 = 0.9991	5	10	8.1 %
	Standard addition	y = 4.0083x + 182.33	R^2 = 0.9944	10	25	
Vincristine	External calibration	y = 3.3054x	R^2 = 0.9998	5	10	10.0 %
	Standard addition	y = 3.6450x + 294.39	R^2 = 0.9954	10	25	

consequences on the growth, the authors suggested the utilization of UV light only for a short period before harvest. Our experiment demonstrated that a 2-week-long application of blue light can also provide similar efficiency as the UV treatment. These results supported that the short wavelength of light can also stimulate the synthesis of these alkaloids.

Multivariate statistical analyses were carried out for both the 2-fold diluted and the 10-fold diluted samples as well to match the dynamic range of the UPLC-ESI-QTOF-MS set-up. The PCA analysis could successfully discriminate group No. 1 in the case of the 2-fold diluted and the 10-fold diluted samples as well (see Figs. 6 and 7, respectively), but group No. 4 (control group) was not clearly distinguished from the other experimental groups. To highlight the metabolic changes induced by blue light, variable importance of projection (VIP) statistics for the modeling coefficients of PLS-DA were determined. Taking into account the ANOVA results and the higher abundance of key compounds in experimental groups No. 1 and 4 (high blue and control conditions, respectively), these two groups were included in the PLS-DA, S-plot and VIP statistics. In these, 4858 metabolites were encountered in the positive ion mode analysis. Compounds with a VIP score > 2 were regarded

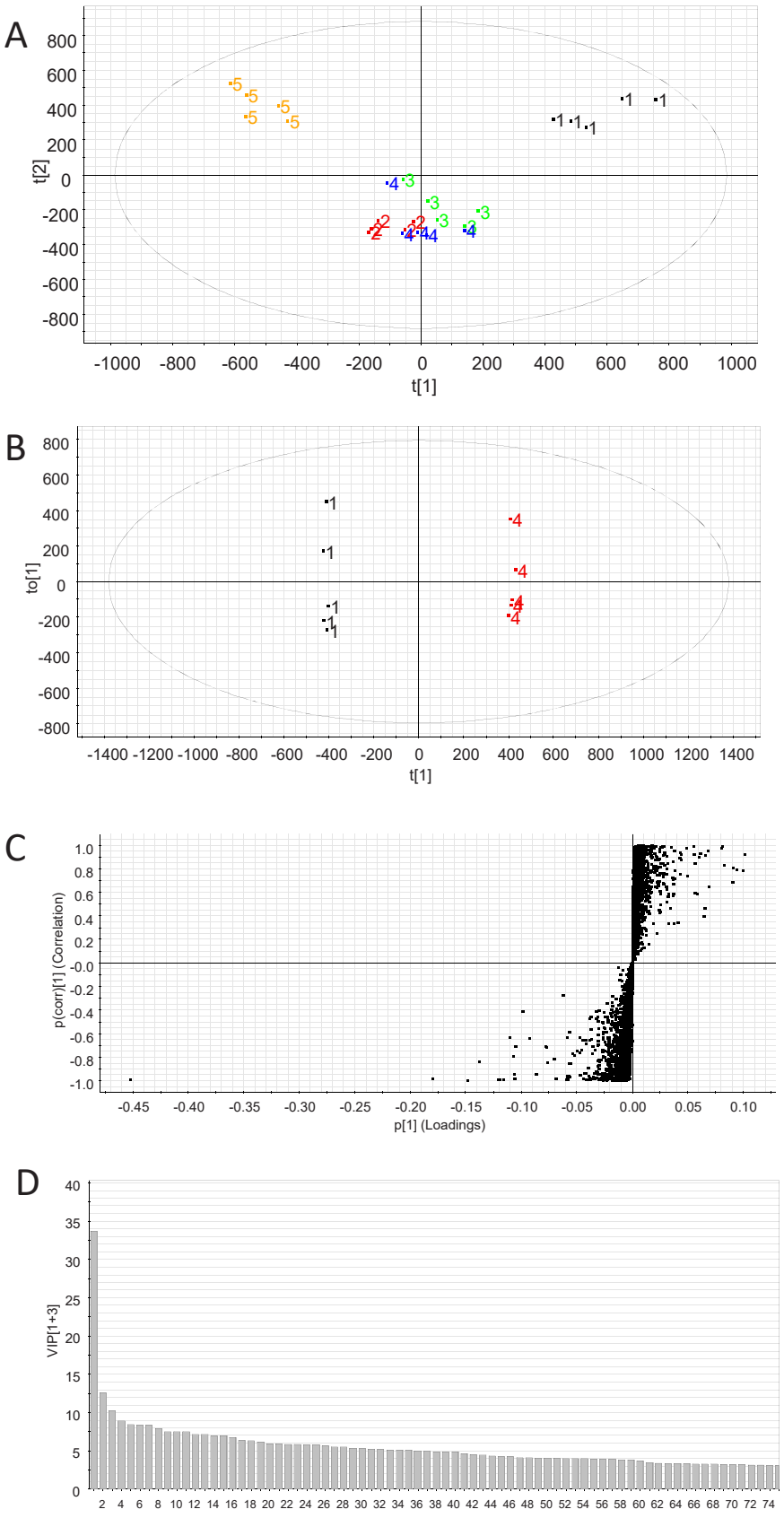

Fig. 6. Multivariate statistical analyses of the 2-fold diluted sample extracts. A – PCA; B – PLS-DA; C – S-plot; D – Variable Importance (VIP) scores.

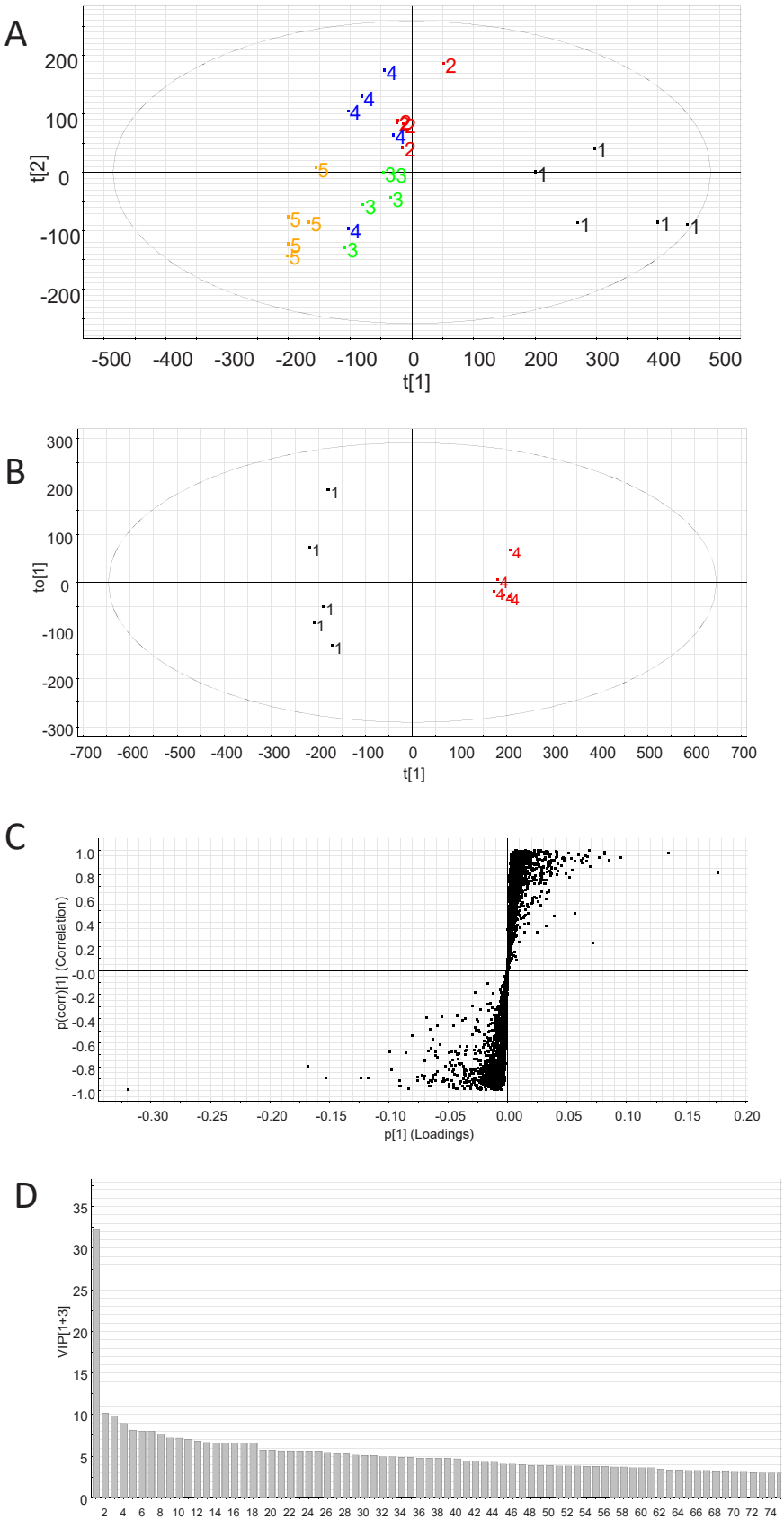

Fig. 7. Multivariate statistical analyses of the 10-fold diluted sample extracts. A – PCA; B – PLS-DA; C – S-plot; D – Variable Importance (VIP) scores.

Table 7
Average concentrations of 3'4'-anhydrovinblastine, vinblastine and vincristine in the five experimental groups (± 1 SD).

No.	Concentration (mg kg^{-1} dry weight) 3',4'-Anhydrovinblastine	Vinblastine	Vincristine
1	961 ± 137	33.8 ± 4.71	11.7 ± 0.85
2	69.9 ± 8.50	2.68 ± 0.26	0.59 ± 0.11
3	123 ± 28.8	4.38 ± 0.85	0.92 ± 0.13
4	83.0 ± 15.7	3.66 ± 0.46	0.78 ± 0.12
5	337 ± 119	15.1 ± 4.51	4.44 ± 1.50

as the most contributory variables, and 165 compounds exceeded this limit. When comparing the control group (group No. 4) with the group No. 1 (high blue), the two most important vinca alkaloids (vinblastine, vincristine), their direct precursors, namely, catharanthine, vindoline, and finally, 3',4'-anhydrovinblastine (this latter one with the highest VIP score /32.3/ among the 165 metabolites) proved to be highly discriminative in groups No. 1 (high blue) (Table 5). The results indicated that the key metabolites of the vinca alkaloid pathway were highly represented among the metabolites that were specifically stimulated by high blue light application. These VIP scores should anyhow be regarded in the view of the Games-Howell's post hoc test results to match the discriminative power with the abundance / concentration data; accordingly, the high blue LED application was finally responsible for the significant enrichment of four vinca alkaloids, that is, vinblastine, vincristine, 3',4'-anhydrovinblastine and vindolinine (ESI-Table S1). The final concentration ranges are presented in Table 7 and ESI-Fig. 31 (961 mg kg^{-1} DW, 33.8 mg kg^{-1} DW and 11.7 mg kg^{-1} DW for 3',4'-anhydrovinblastine, vinblastine and vincristine, respectively). However, the concentration levels of vincristine and vinblastine reported in the literature cannot be always compared with our study in a straightforward manner due to either different production schemes (e.g., callus culture) or analytical approaches, the concentration of vinblastine in the high blue light group exceeds some of the recently published levels in screening studies (13.1 mg kg^{-1} DW, Mujib et al. [32]) and even after UV-A irradiation (2–30 mg kg^{-1} DW; Fukuyama et al., 2017 [13]), which is also valid for vincristine (4.22 mg kg^{-1} DW, Mujib et al. [32]).

The light-dependent regulation of the synthesis of indole alkaloids is poorly understood. Comparing etiolated and light-treated *C. roseus* seedlings, Vazquez-Folta and Luca [33] demonstrated the participation of photoreversible phytochromes in the regulation of the enzymes responsible of vindoline biosynthesis at gene expression level. Red light treatment promoted, while far-red light reversed these effects. Some transcriptional factors, such as GATA and PIF were identified in the regulatory pathway responsible for the vindoline and vinblastine synthesis, but the blue-light-induced accumulation of these metabolites is not yet known. According to Zhu et al. [31], UV-B radiation also increased the indol alkaloids in *C. roseus*, meanwhile most of the structural genes in alkaloid biosynthetic pathway were upregulated. Although detailed analysis has not been performed yet, it is likely, that UV and or blue light photoreceptors are also involved in these processes. Our results supported this hypothesis; however, further investigations are required for the identification of blue-light mediated photoreceptors involved in vindoline and vinblastine synthesis. This is especially important as the dimerization (formation) of 3',4'-anhydrovinblastine is often regarded as a bottleneck in the synthesis (and evidently, when aiming at the high production yield) of vinblastine and vincristine [34], and our experiments revealed this bottleneck might be eliminated by the application of blue light irradiation.

4. Conclusions

The biosynthesis of indole alkaloids in *C. roseus* plants has been studied comprehensively in a set of experiments under different LED illumination conditions. Out of the metabolites of the related pathway, 14 analytes could be assigned with the help of the UPLC-ESI-QTOF-MS setup in the samples, and the concentrations of three alkaloids, vinblastine, vincristine, and 3',4'-anhydrovinblastine were quantified. While none of the experimental settings resulted in a significant increase in plant height, the application of high blue LED conditions significantly, up to 15-fold raised the concentration of these key vinca alkaloids.

Funding

The study was financially supported by the bilateral international research project No. NKM2022-1/2023. of the Hungarian Academy of Sciences (MTA; Hungary) and the Egyptian Academy of Scientific Research and Technology (ASRT; Egypt). The study was supported by the National Research, Development and Innovation Office, Hungary (grant No. K131907).

CRediT authorship contribution statement

Katalin Nagy: Investigation, Writing - Original Draft; **Éva Darkó:** Conceptualization, Methodology; **Gabriella Szalai**: Investigation, Methodology; **Tibor Janda:** Project administration, Supervision; **Zsuzsa Jókai:** Resources, Supervision; **Márta Ladányi:** Visualization, Statistics; **Mohamed Ramadan Rady:** Conceptualization, Funding acquisition; **Mihály Dernovics:** Investigation, Funding acquisition, Writing - Review & Editing.

Declaration of Competing Interest

The authors declare the following financial interests/personal relationships which may be considered as potential competing interests: Mihály Dernovics reports a relationship with the Hungarian Academy of Sciences (MTA) and the Egyptian Academy of Scientific Research and Technology (ASRT) that includes: funding grants and travel reimbursement. Mohamed Ramadan Rady reports a relationship with the Hungarian Academy of Sciences (MTA) and the Egyptian Academy of Scientific Research and Technology (ASRT) that includes: funding grants and travel reimbursement.

Acknowledgements

The Doctoral School of Food Science at the Hungarian University of Agriculture and Life Sciences supported this research. The authors acknowledge Ildikó Denyicska and Tímea Oláh for their technical assistance.

Appendix A. Supporting information

Supplementary data associated with this article can be found in the online version at doi:10.1016/j.jpba.2023.115611.

References

[1] Z. Yaniv, U. Bachrach. Handbook of Medicinal Plants, 1 ed.,, CRC Press,, 2005, https://doi.org/10.1201/9781482278026.
[2] N.R. Farnsworth, in: E.O. Wilson (Ed.), Screening plants for new medicines, Biodiversity, National Academies Press, Washington, D.C, 1988, pp. 83–97, https://doi.org/10.17226/989.
[3] World Health Organization, WHO guidelines on good manufacturing practices (GMP) for herbal medicines, 2007. ISBN: 978 92 4 154716 1.
[4] M. Olle, A. Viršile, The effects of light-emitting diode lighting on greenhouse plant growth and quality, AFSci 22 (2013) 223–234, https://doi.org/10.23986/afsci.7897.
[5] É. Darkó, P. Heydarizadeh, B. Schoefs, M.R. Sabzalian, Photosynthesis under artificial light: the shift in primary and secondary metabolism, Philos. Trans. R. Soc. B 369 (2014) 20130243, https://doi.org/10.1098/rstb.2013.0243.
[6] D. Singh, C. Basu, M. Meinhardt-Wollweber, B. Roth, LEDs for energy efficient greenhouse lighting, Renew. Sust. Energ. Rev. 49 (2015) 139–147, https://doi.org/10.1016/j.rser.2015.04.117.
[7] É. Darkó, K.A. Hamow, T. Marček, M. Dernovics, M. Ahres, G. Galiba, Modulated light dependence of growth, flowering, and the accumulation of secondary

metabolites in chilli, Front. Plant Sci. 13 (2022), 801656, https://doi.org/10.3389/fpls.2022.801656.
[8] P. Kubica, A. Szopa, B. Prokopiuk, Ł. Komsta, B. Pawłowska, H. Ekiert, The influence of light quality on the production of bioactive metabolites – verbascoside, isoverbascoside and phenolic acids and the content of photosynthetic pigments in biomass of *Verbena officinalis* L. cultured *in vitro*, J. Photochem. Photobiol. B 203 (2020) 111768, https://doi.org/10.1016/j.jphotobiol.2019.111768.
[9] P. Vici, G. Colucci, V. Gebbia, A. Amodio, F. Giotta, F. Belli, F. Conti, N. Gebbia, G. Pezzella, M.R. Valerio, M. Brandi, S. Pisconti, E. Durini, D. Giannarelli, M. Lopez, First-line treatment with epirubicin and vinorelbine in metastatic breast cancer, Clin. Oncol. 20 (2002) 2689–2694, https://doi.org/10.1200/JCO.2002.06.039.
[10] S. Kumar, B. Singh, R. Singh, *Catharanthus roseus* (L.) G. Don: a review of its ethnobotany, phytochemistry, ethnopharmacology and toxicities, J. Ethnopharmacol. 284 (2022), 114647, https://doi.org/10.1016/j.jep.2021.114647.
[11] T. Fukuyama, K. Ohashi-Kaneko, E. Ono, H. Watanabe, Growth and alkaloid yields of *Catharanthus roseus* (L.) G. Don cultured under red and blue LEDs, Shokubutsu Kankyo Kogaku 25 (2013) 175–182, https://doi.org/10.2525/shita.25.175.
[12] T. Fukuyama, K. Ohashi-Kaneko, H. Watanabe, Estimation of optimal red light intensity for production of the pharmaceutical drug components, vindoline and catharanthine, contained in *Catharanthus roseus* (L.) G. Don, Environ. Control. Biol. 53 (2015) 217–220, https://doi.org/10.2525/ecb.53.217.
[13] T. Fukuyama, K. Ohashi-Kaneko, K. Hirata, M. Muraoka, H. Watanabe, Effects of ultraviolet a supplemented with red light irradiation on vinblastine production in *Catharanthus roseus*, Environ. Control. Biol. 55 (2017) 65–69, https://doi.org/10.2525/ecb.55.65.
[14] Z. Zhong, S. Liu, S. Han, Y. Li, M. Tao, A. Liu, Q. He, S. Chen, C. Dufresne, W. Zhu, J. Tian, Integrative omic analysis reveals the improvement of alkaloid accumulation by ultraviolet-B radiation and its upstream regulation in *Catharanthus roseus*, Ind. Crops Prod. 166 (2021), 113448, https://doi.org/10.1016/j.indcrop.2021.113448.
[15] Q. Chen, Z. Chen, Analysis of Catharanthus Alkaloids, in: K.G. Ramawat, J.-M. Mérillon, (Eds.), Natural Products, Springer Berlin Heidelberg, Berlin, Heidelberg, 2013, pp. 1121–1132. https://doi.org/10.1007/978–3-642–22144-6_33.
[16] M.S.C. Lourenço, J.E.C. Prada, E. Heuvelink, S.M.P. Carvalho, Production of *Catharanthus roseus* in vertical farming systems: dynamic analyses of plant morphological responses of nine cultivars to N-UV supplementation, in: Acta Hortic, 1337, 2022, pp. 217–224, https://doi.org/10.17660/ActaHortic.2022.1337.29.
[17] S. Hisiger, M. Jolicoeur, Analysis of *Catharanthus roseus* alkaloids by HPLC, Phytochem. Rev. 6 (2007) 207–234, https://doi.org/10.1007/s11101-006-9036-y.
[18] N. Kulagina, L.-V. Méteignier, N. Papon, S.E. O'Connor, V. Courdavault, More than a *Catharanthus* plant: a multicellular and pluri-organelle alkaloid-producing factory, Curr. Opin. Plant Biol. 67 (2022), 102200, https://doi.org/10.1016/j.pbi.2022.102200.
[19] S. Kumar, A. Singh, B. Kumar, B. Singh, L. Bahadur, M. Lal, Simultaneous quantitative determination of bioactive terpene indole alkaloids in ethanolic extracts of *Catharanthus roseus* (L.) G. Don by ultra high performance liquid chromatography–tandem mass spectrometry, J. Pharm. Biomed. Anal. 151 (2018) 32–41, https://doi.org/10.1016/j.jpba.2017.12.040.
[20] F. Ferreres, D.M. Pereira, P. Valentão, J.M.A. Oliveira, J. Faria, L. Gaspar, M. Sottomayor, P.B. Andrade, Simple and reproducible HPLC–DAD–ESI-MS/MS analysis of alkaloids in *Catharanthus roseus* roots, J. Pharm. Biomed. Anal. 51 (2010) 65–69, https://doi.org/10.1016/j.jpba.2009.08.005.
[21] W.T. Jeong, H.B. Lim, A. UPLC-ESI-Q-TOF, method for rapid and reliable identification and quantification of major indole alkaloids in *Catharanthus roseus*, J. Chromatogr. B 1080 (2018) 27–36, https://doi.org/10.1016/j.jchromb.2018.02.018.
[22] M. Al-Amin, N.M. Eltayeb, S.S.F. Rahiman, M. Khairuddean, S.M. Salhimi, UPLC-ESI-QTOF-MS/MS and ^{1}H NMR identification of alkaloids in potent fraction of *Catharanthus roseus* leaves inhibits migration and invasion of MDA-MB-231 cells, Biologia 77 (2022) 3291–3303, https://doi.org/10.1007/s11756-022-01185-6.
[23] B. Yu, Y. Liu, J. Liu, X. Guo, Z. Tang, Integrated analyses of metabolomic profiling and associated gene expression of *Catharanthus roseus* seedling reveal the metabolic alternations of primary metabolites and flavonoids during the apical hook opening phase, J. Plant Growth Regul. 41 (2022) 2093–2107, https://doi.org/10.1007/s00344-021-10374-7.
[24] T. Tan, S. Li, Y. Fan, Z. Wang, M. Ali Raza, I. Shafiq, B. Wang, X. Wu, T. Yong, X. Wang, Y. Wu, F. Yang, W. Yang, Far-red light: a regulator of plant morphology and photosynthetic capacity, Crop J. 10 (2022) 300–309, https://doi.org/10.1016/j.cj.2021.06.007.
[25] MoNA - MassBank of North America. https://mona.fiehnlab.ucdavis.edu/ (accessed on May 25, 2023).
[26] S. Kumar, A. Singh, V. Bajpai, M. Srivastava, B.P. Singh, B. Kumar, Structural characterization of monoterpene indole alkaloids in ethanolic extracts of *Rauwolfia* species by liquid chromatography with quadrupole time-of-flight mass spectrometry, J. Pharm. Anal. 6 (2016) 363–373, https://doi.org/10.1016/j.jpha.2016.04.008.
[27] S. Abouzeid, U. Beutling, F. Surup, F.M.A. Bar, M.M. Amer, F.A. Badria, M. Yahyazadeh, M. Brönstrup, D. Selmar, Treatment of Vinca minor leaves with methyl jasmonate extensively alters the pattern and composition of indole alkaloids, J. Nat. Prod. 80 (2017) 2905–2909, https://doi.org/10.1021/acs.jnatprod.7b00424.
[28] Z. Wang, Y. Xiao, S. Wu, J. Chen, Deciphering and Reprogramming the Cyclization Regioselectivity in Bifurcation of Indole Alkaloids Biosynthesis, Chem. Sci. 13 (42) (2022), https://doi.org/10.1039/D2SC03612F.
[29] Q. Pan, C. Wang, Z. Xiong, H. Wang, X. Fu, Q. Shen, B. Peng, Y. Ma, X. Sun, K. Tang, CrERF5, an AP2/ERF transcription factor, positively regulates the biosynthesis of bisindole alkaloids and their precursors in *Catharanthus roseus*, Front. Plant Sci. 10 (2019) 931, https://doi.org/10.3389/fpls.2019.00931.
[30] J.G.M. Eng, M. Shahsavarani, D.P. Smith, J. Hájíček, V. De Luca, Y. Qu, A *Catharanthus roseus* Fe(II)/α-ketoglutarate-dependent dioxygenase catalyzes a redox-neutral reaction responsible for vindolinine biosynthesis, Nat. Commun. 13 (2022) 3335, https://doi.org/10.1038/s41467-022-31100-1.
[31] R. Yu, J. Zhu, M. Wang, W. Wen, Biosynthesis and regulation of terpenoid indole alkaloids in *Catharanthus roseus*, Pharm. Rev. 9 (2015) 24, https://doi.org/10.4103/0973-7847.156323.
[32] A. Mujib, S. Fatima, M.Q. Malik, Cryo-derived plants through embryogenesis showed same levels of vinblastine and vincristine (anticancer) in *Catharanthus roseus* and had normal genome size, Sci. Rep. 12 (2022) 16635, https://doi.org/10.1038/s41598-022-20993-z.
[33] F.A. Vazquez-Flota, V. De Luca, Developmental and light regulation of desacetoxyvindoline 4-hydroxylase in *Catharanthus roseus* (L.) G. Don, Plant Physiol. 117 (1998) 1351–1361, https://doi.org/10.1104/pp.117.4.1351.
[34] M. Asano, K. Harada, A. Umeno, K. Hirata, Optimization of 3', 4'-anhydrovinblastine synthesis in vitro using crude extracts of *Catharanthus roseus* irradiated with near-ultraviolet light, Nat. Prod. Commun. 11 (8) (2016) 1089–1092, https://doi.org/10.1177/1934578X1601100814.
[35] KEGG Indole alkaloid biosynthesis - Reference pathway. https://www.kegg.jp/pathway/map00901 (accessed on May 25, 2023).